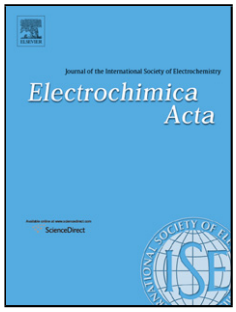

Title: Catecholamine-Functionalised Reduced Graphene Oxide: A Scalable Carbon Host for Stable Cycling in Lithium–Sulfur Batteries

Authors: Syed Abdul Ahad, P. Ramesh Kumar, Joo-Hyung Kim, Dong Jun Kim, P. Ragupathy, Do Kyung Kim

PII: S0013-4686(17)31280-X
DOI: http://dx.doi.org/doi:10.1016/j.electacta.2017.06.042
Reference: EA 29680

To appear in: *Electrochimica Acta*

Received date: 27-2-2017
Revised date: 31-5-2017
Accepted date: 6-6-2017

Please cite this article as: Syed Abdul Ahad, P.Ramesh Kumar, Joo-Hyung Kim, Dong Jun Kim, P.Ragupathy, Do Kyung Kim, Catecholamine-Functionalised Reduced Graphene Oxide: A Scalable Carbon Host for Stable Cycling in Lithium–Sulfur Batteries, Electrochimica Actahttp://dx.doi.org/10.1016/j.electacta.2017.06.042

Catecholamine-Functionalised Reduced Graphene Oxide: A Scalable Carbon Host for Stable Cycling in Lithium–Sulfur Batteries

Syed Abdul Ahad, [a] *P. Ramesh Kumar,* [a] *Joo-Hyung Kim,* [a] *Dong Jun Kim,* [b] *P. Ragupathy,* [a, c] *Do Kyung Kim* [a]*

[a] Department of Materials Science and Engineering, Korea Advanced Institute of Science and Technology (KAIST), Daejeon 34141, Republic of Korea

[b] Department of Chemistry, Northwestern University, Evanston, IL

[c] Electrochemical Power Sources Division, Fuel Cells Section, Central Electrochemical Research Institute, Karaikudi-630 003, India

*Corresponding author: dkkim@kaist.ac.kr

Abstract

The Lithium–Sulfur battery is a promising high performance battery candidate for large-scale application on account of its high theoretical specific capacity. However, it has come up short on delivering long cycle life mainly due to the formation of soluble polysulfides, which results in the loss of active material during redox processes. In this study, we prepared three different graphene oxide based carbon hosts – graphene oxide (GO), thermally reduced GO (t-rGO) and dopamine-assisted chemically reduced GO (c-rGO) – and investigated their physical and electrochemical properties as a sulfur cathode. We found significant absorbance of polysulfides on the c-rGO host, which provided stable discharge capacity of 601 mAh g^{-1} at 0.5 C for up to 300 cycles. This stable cycling behaviour is further identified by *in-situ* UV-Vis spectroscopy and *ex-situ* X-ray photoelectron spectroscopy, confirming the minimization of polysulfide dissolution toward the electrolyte through the adsorption of polydopamine coating.

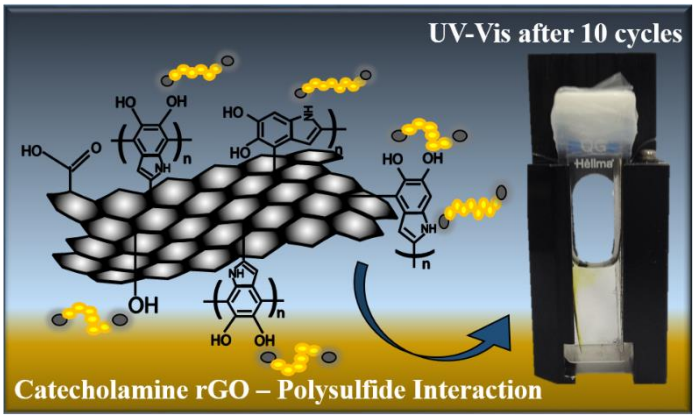

Keywords: Lithium-Sulfur battery, polydopamine, chemically reduced graphene oxide, polysulfide, *in-situ* UV-Vis spectroscopy

1. Introduction

The demands for storing renewable energy and fuel for electric vehicles are growing rapidly, and the developing advanced energy storage devices are important scientific challenges. Among the current battery technologies, the Lithium-Sulfur (Li–S) battery has been considered as one of the promising candidates on account of its exceptionally high theoretical specific capacity of 1675 mAh g^{-1} as well as its power density of 2500 Wh kg^{-1}, compared with the lithium-ion battery system [1];[2]**.** Furthermore, elemental sulfur's high abundance, low toxicity and cost ($30 / ton) are other advantages for designing large-scale energy storage for electrical vehicles [3]; [4]; [5]. Nonetheless, the Li–S battery system needs to overcome a low cycle life problem in order to satisfy the state of art energy storage applications. A major reason for the low cyclability of the Li–S battery is that the formation of lithium polysulfides (Li_2S_x, $2 < x < 8$) during electrochemical cycling causes dissolution of the active material in the sulfur cathode over the cycles [6]; [7]; [8]. Moreover, the low electronic conductivity of sulfur ($5x10^{-30}$ S cm^{-1}) as well as the large volume expansion during cell cycling (~ 80%) are other important issues to consider when designing long cycle life sulfur composite electrodes [9]; [10].

Recently, significant efforts have been directed toward encapsulation of polysulfides from the electrode and increase in the electronic conductivity using various carbon templates, for example, incorporating nanostructured carbon frameworks such as micro/mesoporous carbon [11] graphene oxide (GO) / graphene sheets [12]; [13]; [14], carbon nanofibers/nanotubes [15]; [16], three dimensional carbon and metal foams, to simultaneously provide better electron transport through a sulfur cathode[17]; [18]. In many cases, however, the polysulfides diffuse out from the carbon framework during extended battery cycling because of the different nature of surface polarity [19]. This mismatch in surface properties has been addressed by introducing polar frameworks or polymer coating in the cathode [20]; [21]; [22]; [23]; [24]; [25]. A downside of using polar oxides or polymeric materials is the insulating properties of these additives that decrease the overall electronic conductivity of the cathode components. Therefore, it is important to have a functionalised framework which prevents dissolution of polysulfides and maintains electrical conductivity.

Among many carbon hosts, graphene offers high mechanical and superior electrochemical stability along with improved ionic and electronic transport through a shorter diffusion pathways [26]. In addition to graphene having better electronic transport, polar interactions with lithium polysulfides have been reported in a graphene oxide (GO)-sulfur composite. The interaction between hydroxyl and epoxide functionalities with soluble polysulfides has been reported to depreciate the polysulfide dissolution into the electrolyte [27]. However, GO has numerous functional groups (hydroxyl, epoxide, carbonyl and carboxylic) on its surface which lowers its electronic conductivity [28]. To address this issue, various reduced graphene oxide (rGO) and/or graphene-sulfur composites have been proposed [29]. However rGO and/or graphene do not have any significant functional groups on its surface to chemically interact with polysulfides and prevent them from dissolution. Various strategies, such as using hydroxylated graphene-sulfur and amino functionalised reduced graphene oxides-sulfur

composites have been proposed where the hydroxyl and amino groups bind the polysulfides while the graphene backbone is effective in improving electronic conductivity. However, these impressive studies achieved a sulfur content of not more than 70 wt. % thus limiting the practical applicability for the Li-S battery. Moreover, the use of hydrothermal processes and the toxic chemicals like ethylene diamine (EDA) is also a hindrance in scaling-up the process for commercialisation of Li-S batteries [30]; [31]. Undoubtedly, still much work has to be done to develop and explore environmental friendly approaches to reduce graphene oxide with tailored properties targeting polysulfide entrapment at the cathode site. We suggest that the conductivity issue can be resolved using functionalised carbon framework which can provide better electrical conductivity as well as polysulfide entrapment through functional groups attached to the carbon host.

It has been previously reported that dopamine, a mussel inspired biomolecule having both adhesive and hydrophilic characteristics can simultaneously reduce and functionalise GO [32]; [33]. Upon the reaction of dopamine with GO under weak alkaline conditions and in the presence of dissolved O_2, dopamine undergoes oxidative polymerization and can self-polymerize to polydopamine (PDA), thus modifying the GO surface with catechol and amine functionalities. Besides facile preparation and functionalisation, dopamine can reduce GO to rGO since polydopamine (PDA) is a semiconductor which can repair rGO defects and thus enhance its electrical conductivity by π - π stacking [34]; [35]. Previously, a few reports that achieved better cyclic performance and DFT calculations suggested the possibility of polysulfide interaction with polydopamine [36]; [37]. This inspired us to use polydopamine functionalities and specifically tailor the properties of GO, to take advantage of the benefit of both better electrical conductivity and catecholamine-polysulfide interaction.

Here, we report a simple and environmental friendly approach to preparing a reduced graphene-sulfur composite electrode with hydrophilic surface properties. For this experiment,

we used 3,4-dihydroxyphenethylamine – also known as dopamine – as a reducing agent and monomer unit for polydopamine coating. The synthesised dopamine based sulfur (c-rGOS) composite demonstrated superior discharge capacity as well as cyclability compared to the graphene oxide-sulfur composite (GOS) and thermally reduced graphene oxide-sulfur composite (t-rGOS). In addition, the improved cyclability of c-rGOS was further supported by *in-situ* UV-Vis spectroscopy. Our results highlight the importance of designing the surface of sulfur composites.

The synthesised dopamine based sulfur composite (c-rGOS) had a stable discharge capacity of 601 mAh g^{-1} after 300 cycles at a current rate of 0.5 C, as compared to the poor cyclability of the graphene oxide-sulfur composite (GOS) and the thermally reduced graphene oxide-sulfur composite (t-rGOS). The catecholamine-polysulfide binding effect by carrying out *in-situ* UV-Vis spectroscopy explained the c-rGOS composite's stable discharge capacity as compared to the poor cyclic performance of GOS and t-rGOS.

2. Results and Discussion

2.1. Microstructural Analysis

Fig. 1 focuses on the synthesis route of c-rGO and summarizes the possible interaction of polysulfides with GO, t-rGO and c-rGO carbon hosts. The c-rGO carbon host was synthesized using a one-step chemical reduction process. Briefly, dopamine hydrochloride and Tris buffer solution (pH = 8.5) was added to the GO solution followed by vigorously stirring at 80 °C for 24 h yielding a black solution of c-rGO. The c-rGO solution was filtered and freeze-dried followed by sulfur infiltration at 155 °C for 12 h in an Ar gas sealed container. Unlike the hydrothermal process previously used to synthesis functionalised graphene, the current route is simple and scalable since the c-rGO synthesis involves stirring in air only [30]. Additionally, dopamine is a non-toxic organic compound, thus its use to reduce GO is non-hazardous, which

is unlike many other toxic reducing agents, such as hydrazine and ethylene diamine (EDA) [31]; [38]. Though GOS has functional groups like hydroxyl and epoxide functionalities which assist in polysulfide adsorption, the lower electronic conductivity of oxidized species lessens the active material utilisation and thus has a poor capacity [27]. For comparison, the t-rGO carbon host with almost no surface functional groups was also synthesized to highlight that providing only better electronic conductivity to a sulfur cathode cannot guarantee stable discharge capacity unless polysulfide adsorption groups are present on the t-rGO surface [39]. The c-rGO carbon host, upon chemical reduction provides improved electronic conductivity and addition of effective catecholamine functional groups which helps in providing better active material utilization as well as polysulfide entrapment; thus, the c-rGO carbon host delivers a stable discharge capacity as compared to the GO and t-rGO hosts when in a sulfur cathode composite for Li-S battery.

The thermal and chemical reductions of GO were confirmed through XRD analysis and are summarized in Fig. S1 (a). The GO reference peak at 11° shifts to ~25° for t-rGO and c-rGO carbon hosts, which correspond a decrease in d-spacing from GO (0.79 nm) to c-rGO (0.32 nm), and suggests the successful removal of oxygen functionalities from the GO surface. The broad nature of peaks in t-rGO and c-rGO carbon host shows that the typical π-π stacking of graphene sheets is prevented after both thermal and chemical reduction [40]. After sulfur infiltration, the XRD analysis (Fig. 2 (a)) shows diffraction peaks corresponding to the sulfur orthorhombic phase (JCPDS no. 08-0247) and confirming the presence of crystallized sulfur in all three composites, GOS, t-rGOS and c-rGOS.

The various functional groups present on GO, t-rGO and c-rGO carbon hosts were investigated by using XPS and FTIR analysis. The XPS analysis highlights the presence of functional groups before and after GO reduction process. The GO high resolution C 1s spectra (Fig. S1 (c)) show peaks corresponding to C-C/C=C, C=O and O-C=O groups while the t-rGO C 1s

spectra (Fig. S1 (d)) verifies the removal of oxygen functionalities by showing significant decrease in C-O, C=O and O-C=O peak intensities. After chemical reduction by dopamine, the c-rGO high resolution C 1s spectra (Fig. 2 (b)) shows a significant reduction in C-O, C=O and O-C=O peak intensity, whereas a new peak corresponding to a C-N/C-OH species appears at 285.8 eV, thus confirming the successful reduction of GO to c-rGO with further addition of polydopamine on the c-rGO surface [41]. The XPS results of the GO, t-rGO and c-rGO composites are well supported by the FTIR results presented in Fig. S1 (b). Even after sulfur infiltration, the amino functionalities are well present in the c-rGOS composite as evident by the C 1s spectra of the c-rGOS composite presented in Fig. 2 (c). The corresponding N 1s and S 2p spectra of the c-rGOS composite (Fig. S2 (a) and (b)) show pyrrolic N (~399.5 eV) and elemental sulfur (163.7 eV – 165 eV) in the final c-rGOS cathode composite. The material characterization done by XRD, XPS and FTIR suggests successful synthesis of reduced graphene oxide by chemical and thermal reduction methods along with their sulfur composites.

The morphological study of the carbon hosts and their respective sulfur infiltrated cathode composites was carried out using transmission electron microscopy (TEM). The TEM images of GO, t-rGO and c-rGO carbon hosts (Fig. S3 (a) - (c)) reveal the presence of several micrometer long sheets of crumpled and wrinkled graphene. After sulfur infiltration, the c-rGOS, GOS and t-rGOS TEM analysis reveals a similar crumpled morphology (Fig. 2 (a) & Fig. S4 (a-b)) as found in its carbon host. The TEM elemental mapping of the c-rGOS composite (Fig. 2 (b)) confirms uniform distribution of sulfur on the c-rGO sheet suggesting that sulfur has been uniformly coated on the graphene sheets using a melt diffusion method. Not only sulfur but N and O elements coming from catecholamine group in polydopamine are also well distributed on the c-rGO sheet, which additionally confirms the prior uniform functionalisation of polydopamine on the c-rGO carbon host. The elemental analysis results presented in Table 1 (See Supplementary data) suggests a sulfur content of ~74 wt.% in all

three cathode composites. Due to the presence of polydopamine in c-rGOS, the wt.% of O and N elements is highest in c-rGOS contrary to the negligible amount of such elements (especially N) present in the other two sulfur composites (GOS and t-rGOS).

2.2.Electrochemical performance

With an aim of understanding the influence of catecholamine functionalised rGO (c-rGO) in trapping polysulfides, the electrochemical performance was measured. For comparison, GOS and t-rGOS composites were also tested to verify the important role of the c-rGO carbon host in the sulfur composite. For standardization of the electrochemical characterization, ~ 40 µl electrolyte was used while making cell. The average sulfur loading in the composite electrode is ~ 1 mg cm^{-2}. The specific capacity and C-rates are calculated based on the weight of sulfur in the cathode (1C = 1675 mAh g^{-1}). The electrochemical cycling performance of all three composites cycled between 1.0 V to 3.0 V at 0.5C is shown in Fig. 3 (a). After pre-cycling at 0.1C for two cycles, the GOS and t-rGOS composites showed a discharge capacity of 595 mAh g^{-1} and 676 mAh g^{-1} whereas the c-rGOS composite showed a discharge capacity of 629 mAh g^{-1} after the 1^{st} cycle at 0.5C. The coulombic efficiency of c-rGOS after the first cycle at 0.5C is 100%, whereas the coulombic efficiency in GOS and t-rGOS is as low as 87.3% and 86.5%, respectively. This suggests that both GOS and t-rGOS have done little to trap the polysulfides within its carbon host structure, whereas the high coulombic efficiency obtained in the c-rGOS composite suggests excellent polysulfide adsorption within the catecholamine functionalised c-rGO carbon host.

After long cycling of 300 cycles, the c-rGOS showed a very stable discharge capacity of 601 mAh g^{-1} with an excellent capacity retention of 95.4% and a coulombic efficiency of 94.7%. The stable discharge capacity in c-rGOS is also reflected in its voltage-capacity profile (Fig. 3 (d)) that shows a very stable two-voltage plateau, whereas GOS and t-rGOS composite

displayed a severe capacity fading down to 87 mAh g^{-1} and 211 mAh g^{-1} respectively after 300 cycles. The voltage-capacity profile of GOS (Fig. 3 (b)) shows high polarization and severe capacity drop during the 300 cycles. The t-rGOS voltage-capacity profile (Fig. 3 (c)) shows slightly better performance compared to GOS but still the capacity drop even in the initial 50 cycles is considerably high compared to the c-rGOS composite. Unlike the c-rGOS voltage capacity profile, the prolonged charging evident in both the GOS and t-rGOS charge profiles suggests shuttle phenomena taking place due to the severe polysulfide dissolution. The high electrochemical stability of the c-rGOS composite is also evident in the CV analysis (Fig. S5).

Evidence of the better electronic conductivity of the c-rGOS cathode composite was gathered by performing EIS analysis (Fig. S6) on the fresh Li-S cells. As expected, GOS has the highest R_{ct} value (~165 Ω) suggesting poor electronic conductivity of the GO carbon host. However in c-rGOS, the R_{ct} value (~108 Ω) has decreased suggesting better electronic conductivity than GOS in the fresh cell. It is understandable that the t-rGOS (R_{ct} ~62 Ω) composite shows highest conductivity in the fresh cell owing to the absence of most of the functional groups from its surface, which restores a better electronic structure than the chemically reduced rGO [29]. Until now the c-rGOS composite has shown exceptionally stable cyclic performance at 0.5 C as compared to the GOS and t-rGOS composites. However, the electrochemical stability of the c-rGOS composite is necessary to show its robust performance at higher C-rates. Thus as depicted in Fig. 3 (e) and (f), the rate performance test was conducted at various C rates (0.2 C – 2 C) to evaluate the electrochemical stability of c-rGOS composite. The c-rGOS composite displayed 995 mAh g^{-1}, 654 mAh g^{-1}, 399 mAh g^{-1} and 267 mAh g^{-1} at 0.2 C, 0.5 C, 1 C and 2 C respectively. After switching again to lower C-rates, the discharge capacity obtained at 0.5 C turns out to be 610 mAh g^{-1} with a capacity retention of 93.3 % at 0.5 C. Such high capacity retention proves the robust electrochemical stability of c-rGOS composite at various C-rates even with a high sulfur content of ~74 wt. %.

According to our hypothesis, the stable electrochemical performance in the c-rGOS composite is due to the catecholamine group (in polydopamine), which adsorbs the lithium polysulfides formed during the discharge reaction. To elucidate this point, XPS analysis before and after the first discharge of the c-rGOS composite Li-S cell was taken and analyzed. As emphasized in Fig. 4 (a), the possible polysulfide interaction is with secondary amino as well as with the catechol group. The Li 1s high resolution spectra (Fig. 4 (b)), obtained after 1st discharge suggests the presence of two peaks which can be fitted to Li-S bond at 55.6 eV and Li-N/Li-O bond at 54.7 eV [42]; [43]. The presence of the Li-N / Li-O peak reflects that the catecholamine group in PDA has a strong interaction with the lithium polysulfides formed during the discharge stage. The N 1s spectra (Fig. 4 (c)) after the first discharge shows a shift in the binding energy to lower value as compared to the N 1s binding energy before the first discharge, probably due to the interaction between Li polysulfides and amino functionalities present in polydopamine. Moreover, the S 2p spectra (Fig. 4 (d)) after the first discharge confirms complete conversion of elemental sulfur to lithium sulfides as a shift in binding energy can be noticed from 163.7-165 eV (elemental sulfur) to 161.5-162.7 eV (lithium sulfides) [31]; [44]. The presence of a sulfate peak in the S 2p spectrum might be due to the interaction of Li_2S_x with air while sample handling. Until now it is been claimed that the c-rGOS has a highly stable discharge capacity owing to the polydopamine (catecholamine functionalities) assisted polysulfide adsorption in the c-rGOS composite. However, the only evidence provided is either through electrochemical data or through *ex-situ* XPS analysis. Since XPS is often performed *ex-situ*, it cannot be a true representation of *in-operando* operations of a Li-S cell.

2.3. *In-situ* UV-Vis analysis of c-rGOS, t-rGOS and c-rGOS Li-S cell

At this point it becomes desirable to show better polysulfide adsorption by the c-rGO carbon host through an *in-situ* characterization technique. We designed an *in-situ* cuvette based UV-

Vis Li-S cell such that the polysulfide dissolution can be monitored during the galvanostatic charge-discharge test. The schematic illustration of the designed *in-situ* cell is shown in Fig. 5 (a). The quartz cuvette based cell fabricated and sealed in an Ar filled glove box comprises Li metal as the anode, composite slurry (GOS, t-rGOS and c-rGOS) as the cathode and 1 M LiTFSI salt in DOL: DME solvent as the electrolyte. The UV-Vis spectrum is obtained in the transmittance mode and the peak positions are determined by taking the derivative of transmittance graphs. Initially the UV-Vis spectrum is obtained for the fresh cell after which the cell is discharged at several points in relation to the discharge-charge curve of a typical Li-S cell (Fig. S7 (a)).

Before discussing the results, we considered it best to describe the range in which a possible response by the dissolved polysulfides can be detected in the UV-Vis spectrum. Usually the existence of the mixture of various chain-length polysulfides (S_8^{2-} ,S_6^{2-} ,S_4^{2-} & $2S_6^{2-} \rightarrow S_8^{2-} + S_4^{2-}$) in DME: DOL solvent shows a UV-Vis response ranging between 400 – 500 nm. This range also depends on the concentration of polysulfides present in the solvent [45]; [46]; [47]. The results for GOS composite *in-situ* cell are shown in Fig. 5 (b). Initially, at OCV there is no change in the transmittance range known for polysulfide presence in the DOL: DME solvent. As the cell is discharged, it reveals that the transmittance value decreases in the wavelength range of 400-550 nm, which shows that the polysulfides are dissolving in the electrolyte. This change increases and becomes significant once the voltage sweeps towards 1.0 V, showing that the amount of polysulfide dissolution in the electrolyte increases significantly even during the first discharge. When the cell is charged to 3.0 V (Fig. S7 (b)), most of the polysulfides still remain in the electrolyte suggesting that the dissolved polysulfides irreversibly remains in the electrolyte and cause shuttle effect, which is responsible for the severe capacity decay in GOS cathode based Li-S cells. When the cell is further discharged to the 5^{th} and 10^{th} cycles, the amount of polysulfide concentration still increases as shown in Fig. 5 (b). A similar trend is

seen in the t-rGOS composite (Fig. 5 (c)), where the polysulfide dissolution significantly increases as the cell is progressively discharged to 1.0 V. Once charged to 3.0 V (Fig. S7 (c)), the t-rGOS composite shows an increase in the transmittance value, thus indicating the polysulfides converting to sulfur on the cathode site. However, large amount of polysulfides still remains in the solution since 100% transmittance has not been achieved upon complete charge. In t-rGOS after the 5^{th} and 10^{th} cycles, the polysulfide dissolution increases as evidenced by the decrease in the transmittance value shown in Fig. 5 (c). A peak centered around 620 nm appearing in both the GOS and t-rGOS discharge profiles suggests the presence of the $S_3^{\bullet-}$ radical which forms due to the dissociation of S_6^{2-} polysulfide species ($S_6^{2-} \rightarrow S_3^{\bullet-}$) [46]; [48].

Until now both GOS and t-rGOS *in-situ* cells have shown significant dissolution of polysulfides even in the first cycle, which can be ascribed as a reason for severe capacity fading. However, when the c-rGOS composite based *in-situ* cell (Fig. 5 (d)) is discharged up to 1.0 V, little polysulfide dissolution is observed in comparison to the large polysulfide dissolution in the GOS and t-rGOS composites. A $S_3^{\bullet-}$ presence is not detected in c-rGOS due to the absence of peaks at 620 nm suggesting that higher order polysulfides, especially S_6^{2-}, is not dissolved in the electrolyte and has been effectively trapped on the cathode site. When charged to 3.0 V (Fig. S7 (d)), the c-rGOS composite shows complete restoration of the transmittance profile suggesting that the small amount of polysulfides dissolved during discharge have demonstrated reversibility. When discharged to the 5^{th} and 10^{th} cycles, the c-rGOS composite showed a decrease in the transmittance value as compared to its first cycle, but the degree of dissolution is still not significant after the 5^{th} and 10^{th} cycles (Fig. 5 (d)) compared to the GOS and t-rGOS cells.

To clearly identify the regions for the polysulfide dissolution, the derivative of transmittance graphs during the first discharge of GOS, t-rGOS and c-rGOS were obtained and are shown in

Fig. S8. The derivative of transmittance graphs shows the highest dissolution of polysulfides in GOS followed by t-rGOS and the least dissolution is observed in c-rGOS. Moreover, the presence of broad peaks in all three composites suggests the co-existence of various polysulfide species, such as S_8^{2-}, S_6^{2-} and S_4^{2-} by creating an equilibrium between them ($S_6^{2-} \rightarrow S_4^{2-} + S_8^{2-}$). It is worth mentioning here that the UV-Vis spectroscopy technique for *in-situ* measurements in the Li-S cell provides more qualitative evidence for identifying the presence of polysulfides dissolution because the disproportionation reactions in polysulfides results in chain growth or shortening depending upon its changing concentration in the electrolyte [49]. The evidence for polysulfide dissolution in all three composites after the 10^{th} discharge cycle is shown in Fig. 6. In comparison to the fresh cell shown in Fig. 6 (a), the GOS and t-rGOS cells (Fig. 6 (b) and (c)) show severe polysulfide dissolution, whereas the c-rGOS cell (Fig. 6 (d)) shows minimal polysulfide dissolution even after 10 cycles. The highly oxidized form of GO with the presence of many undesirable functional groups (such as carboxyl groups) on the GO surface has done little to adsorb polysulfides, thus causing leaching into the electrolyte. Though t-rGO has a much higher electronic conductivity compared to GO and c-rGO, the absence of any polysulfide adsorption group (hydroxyl and/or amino groups) on the t-rGO surface caused severe polysulfide dissolution. However, the catecholamine group in the polydopamine functionalised c-rGO has chemically adsorbed the polysulfides, thus largely inhibiting polysulfide dissolution into the electrolyte. This may be a major reason for the high and stable discharge capacity obtained in the c-rGOS composite compared to the GOS and t-rGOS composites.

3. Conclusions

We demonstrated a scalable and eco-friendly approach to synthesizing a catecholamine functionalized rGO based sulfur cathode for Li-S batteries. High electrochemical stability was obtained in c-rGOS composite as an electrode material in the Li-S battery. Using the c-rGOS

composite as a cathode, we were able to obtain a stable discharge capacity of 601 mAh g^{-1} at 0.5 C with a capacity retention of ~94.7% after 300 cycles. We presented evidence on the polydopamine-polysulfide interaction using ex-situ XPS analysis and *in-situ* UV-Vis spectroscopy using a specially designed *in-situ* UV-Vis cell in our laboratory. The *in-situ* UV-Vis spectroscopy data reveals almost no polysulfide dissolution in the c-rGOS cell compared to GOS and t-rGOS cells. Based on our experimental results, we strongly believe that the functionalized carbon framework holds a great potential in enhancing the current avenues of capacity stabilization in Li-S batteries.

Acknowledgements

This project was supported by EEWS project (Grant No. N11170059). Ragupathy is grateful to The Korean federation of Science and Technology Societies for financial support through Brain Pool program and CSIR-CECRI for granting him the sabbatical leave.

Appendix - Supplementary data

Experimental Procedure; XRD, FTIR and XPS of GO, t-rGO and c-rGO; XPS of N 1s and S2p of c-rGOS; TEM analysis of GO, t-rGO, c-rGO, GOS and t-rGOS; Elemental analysis results of GOS, t-rGOs and c-rGOS measured using elemental analyzer; CV and EIS analysis of GOS, t-rGOS and c-rGOS; In-situ UV-VIS spectrum during 1st charge of GOS, t-rGOs and c-rGOS; Derivative of transmittance profile of GOS, t-rGOs and c-rGOS during 1st discharge.

References

[1] A. Rosenman, E. Markevich, G. Salitra, D. Aurbach, A. Garsuch, F.F. Chesneau, Review on Li-Sulfur Battery Systems: An Integral Perspective, Adv. Energy Mater. 5 (2015) 1–21.

[2] H.W. Lee, P. Muralidharan, R. Ruffo, C.M. Mari, Y. Cui, D.K. Kim, Ultrathin spinel LiMn2O4 nanowires as high power cathode materials for Li-ion batteries, Nano Lett. 10 (2010) 3852–3856.

[3] P.G. Bruce, S. a. Freunberger, L.J. Hardwick, J.-M. Tarascon, Li–O2 and Li–S batteries with

high energy storage, Nat. Mater. 11 (2011) 172–172.

[4] J. Xu, S. Dou, H. Liu, L. Dai, Cathode materials for next generation lithium ion batteries, Nano Energy. 2 (2013) 439–442.

[5] X. Ji, L.F. Nazar, Advances in Li–S Batteries, J. Mater. Chem. 20 (2010) 9821.

[6] R. Xu, I. Belharouak, X. Zhang, R. Chamoun, C. Yu, Y. Ren, A. Nie, R. Shahbazian-yassar, J. Lu, J.C.M. Li, K. Amine, Insight into Sulfur Reactions in Li − S Batteries, ACS Appl. Mater. Interfaces. 6 (2014) 2458–2463.

[7] R. Chen, T. Zhao, F. Wu, From historic review to horizon beyond: Lithium-Sulphur batteries run on the wheels, Chem. Commun. 51 (2014) 18–33.

[8] S. Das, P. Ngene, P. Norby, T. Vegge, P.E. De Jongh, D. Blanchard, All-Solid-State Lithium-Sulfur Battery based on a nanoconfined $LiBH_4$ Electrolyte, J. Electrochem. Soc. 163 (2016) 2029–2034.

[9] Y.X. Yin, S. Xin, Y.G. Guo, L.J. Wan, Lithium-sulfur batteries: Electrochemistry, materials, and prospects, Angew. Chemie - Int. Ed. 52 (2013) 13186–13200.

[10] C.N. Lin, W.C. Chen, Y.F. Song, C.C. Wang, L.D. Tsai, N.L. Wu, Understanding dynamics of polysulfide dissolution and re-deposition in working lithium-sulfur battery by in-operando transmission X-ray microscopy, J. Power Sources. 263 (2014) 98–103.

[11] X. Ji, K.T. Lee, L.F. Nazar, A highly ordered nanostructured carbon-sulphur cathode for lithium-sulphur batteries., Nat. Mater. 8 (2009) 500–506.

[12] C.H.. Lim, A.G.. Kannan, H.-W.. Lee, D.K.. Kim, A high power density electrode with ultralow carbon via direct growth of particles on graphene sheets, J. Mater. Chem. A. 1 (2013) 6183–6190.

[13] S. Moon, Y.H. Jung, D.K. Kim, Enhanced electrochemical performance of a crosslinked polyaniline-coated graphene oxide-sulfur composite for rechargeable lithium-sulfur batteries, J. Power Sources. 294 (2015) 386–392.

[14] Z. Sun, J. Zhang, L. Yin, G. Hu, R. Fang, H.-M. Cheng, F. Li, Conductive porous vanadium nitride/graphene composite as chemical anchor of polysulfides for lithium-sulfur batteries, Nat. Commun. 8 (2017) 14627.

[15] L. Ji, M. Rao, S. Aloni, L. Wang, E.J. Cairns, Y. Zhang, Porous carbon nanofiber–sulfur composite electrodes for lithium/sulfur cells, Energy Environ. Sci. 4 (2011) 5053.

[16] S. Moon, Y.H. Jung, W.K. Jung, D.S. Jung, J.W. Choi, D.K. Kim, Encapsulated monoclinic

sulfur for stable cycling of Li-S rechargeable batteries, Adv. Mater. 25 (2013) 6547–6553.

[17] K. Xi, P.R. Kidambi, R. Chen, C. Gao, X. Peng, C. Ducati, S. Hofmann, R.V. Kumar, Binder free three-dimensional sulphur/few-layer graphene foam cathode with enhanced high-rate capability for rechargeable lithium sulphur batteries, Nanoscale. 6 (2014) 5746.

[18] L.B. Xing, K. Xi, Q. Li, Z. Su, C. Lai, X. Zhao, R.V. Kumar, Nitrogen, sulfur-codoped graphene sponge as electroactive carbon interlayer for high-energy and -power lithium-sulfur batteries, J. Power Sources. 303 (2016) 22–28.

[19] W. Zhou, H. Chen, Y. Yu, D. Wang, Z. Cui, F.J. Disalvo, C. Biology, N. York, U. States, Amylopectin Wrapped Graphene Oxide / Sulfur for Improved Cyclability of Lithium A Sulfur Battery, ACS Nano. 7 (2013) 8801–8808.

[20] Q. Pang, X. Liang, C.Y. Kwok, L.F. Nazar, Review—The Importance of Chemical Interactions between Sulfur Host Materials and Lithium Polysulfides for Advanced Lithium-Sulfur Batteries, J. Electrochem. Soc. 162 (2015) A2567–A2576.

[21] S. Evers, T. Yim, L.F. Nazar, Understanding the Nature of Absorption/Adsorption in Nanoporous Polysul fi de Sorbents for the Li − S Battery, J. Phys. Chem. C. (2012) 19653–19658.

[22] X. Ji, S. Evers, R. Black, L.F. Nazar, Stabilizing lithium-sulphur cathodes using polysulphide reservoirs., Nat. Commun. 2 (2011) 325.

[23] R. Ponraj, A.G. Kannan, J.H. Ahn, D.-W. Kim, Improvement of Cycling Performance of Lithium-Sulfur Batteries by Using Magnesium Oxide as a Functional Additive for Trapping Lithium Polysulfide, ACS Appl. Mater. Interfaces. 8 (6) (2016) 4000–4006.

[24] G.C. Li, G.R. Li, S.H. Ye, X.P. Gao, A Polyaniline-coated sulfur/carbon composite with an enhanced high-rate capability as a cathode material for lithium/sulfur batteries, Adv. Energy Mater. 2 (2012) 1238–1245.

[25] G. Hu, Z. Sun, C. Shi, R. Fang, J. Chen, P. Hou, C. Liu, H.M. Cheng, F. Li, A Sulfur-Rich Copolymer@CNT Hybrid Cathode with Dual-Confinement of Polysulfides for High-Performance Lithium-Sulfur Batteries, Adv. Mater. 29 (2017) 1–6.

[26] A.K. Geim, K.S. Novoselov, The rise of graphene, Nat. Mater. 6 (2007) 183–191.

[27] L. Ji, M. Rao, H. Zheng, L. Zhang, O.Y. Li, W. Duan, Graphene Oxide as a Sulfur Immobilizer in High Performance Lithium/Surfur cells, J. Am. Chem. Soc. 133 (2011) 18522–18525.

[28] Q. Pang, D. Kundu, M. Cuisinier, L.F. Nazar, Surface-enhanced redox chemistry of

polysulphides on a metallic and polar host for lithium-sulphur batteries, Nat Commun. 5 (2014) 4759.

[29] W. Gao, The chemistry of graphene oxide, in: Graphene Oxide Reduct. Recipes, Spectrosc. Appl., 2015: pp. 61–95.

[30] C. Zu, A. Manthiram, Hydroxylated graphene-sulfur nanocomposites for high-rate lithium-sulfur batteries, Adv. Energy Mater. 3 (2013) 1008–1012.

[31] Z. Wang, Y. Dong, H. Li, Z. Zhao, H. Bin Wu, C. Hao, S. Liu, J. Qiu, X.W.D. Lou, Enhancing lithium-sulphur battery performance by strongly binding the discharge products on amino-functionalized reduced graphene oxide., Nat. Commun. 5 (2014) 5002.

[32] Z. Hu, Y. Huang, C. Zhang, L. Liu, J. Li, Y. Wang, Graphene–polydopamine–C 60 nanohybrid: an efficient protective agent for NO-induced cytotoxicity in rat pheochromocytoma cells, J. Mater. Chem. B. 2 (2014) 8587–8597.

[33] R. Gu, W.Z. Xu, P.A. Charpentier, Synthesis of polydopamine-coated graphene-polymer nanocomposites via RAFT polymerization, J. Polym. Sci. Part A Polym. Chem. 51 (2013) 3941–3949.

[34] K. Yang, X. Huang, L. Fang, J. He, P. Jiang, Fluoro-polymer functionalized graphene for flexible ferroelectric polymer-based high-k nanocomposites with suppressed dielectric loss and low percolation threshold, Nanoscale. 6 (2014) 14740–14753.

[35] L. Yang, J. Kong, W.A. Yee, W. Liu, S.L. Phua, C.L. Toh, S. Huang, X. Lu, Highly conductive graphene by low-temperature thermal reduction and in situ preparation of conductive polymer nanocomposites, Nanoscale. 4 (2012) 4968.

[36] Y. Deng, H. Xu, Z. Bai, B. Huang, J. Su, G. Chen, Durable polydopamine-coated porous sulfur core-shell cathode for high performance lithium-sulfur batteries, J. Power Sources. 300 (2015) 386–394.

[37] F. Wu, Y. Ye, R. Chen, J. Qian, T. Zhao, L. Li, W. Li, Systematic Effect for an Ultralong Cycle Lithium-Sulfur Battery, Nano Lett. 15 (2015) 7431–7439.

[38] Z. Bo, X. Shuai, S. Mao, H. Yang, J. Qian, J. Chen, J. Yan, K. Cen, Green preparation of reduced graphene oxide for sensing and energy storage applications., Sci. Rep. 4 (2014) 4684.

[39] Z. Guo, J. Wang, F. Wang, D. Zhou, Y. Xia, Y. Wang, Leaf-like graphene oxide with a carbon nanotube midrib and its application in energy storage devices, Adv. Funct. Mater. 23 (2013) 4840–4846.

[40] Z. Tang, S. Shen, J. Zhuang, X. Wang, Noble-metal-promoted three-dimensional

macroassembly of single-layered graphene oxide, Angew. Chemie - Int. Ed. 49 (2010) 4603–4607.

[41] L. Guo, Q. Liu, G. Li, J. Shi, J. Liu, T. Wang, G. Jiang, A mussel-inspired polydopamine coating as a versatile platform for the in situ synthesis of graphene-based nanocomposites, Nanoscale. 4 (2012) 5864.

[42] D. Aurbach, E. Pollak, R. Elazari, G. Salitra, C.S. Kelley, J. Affinito, On the Surface Chemical Aspects of Very High Energy Density, Rechargeable Li-Sulfur Batteries, J. Electrochem. Soc. 156 (2009) A694–A702.

[43] A.K. Bedyal, V. Kumar, R. Prakash, O.M. Ntwaeaborwa, H.C. Swart, A near-UV-converted $LiMgBO_3:Dy^{3+}$ nanophosphor: Surface and spectral investigations, Appl. Surf. Sci. 329 (2015) 40–46.

[44] L. Ma, H.L. Zhuang, S. Wei, K.E. Hendrickson, M.S. Kim, G. Cohn, R.G. Hennig, L.A. Archer, Enhanced Li–S Batteries Using Amine-Functionalized Carbon Nanotubes in the Cathode, ACS Nano. 10(1) (2015) 1050–1059.

[45] B. Kim, S. Park, In Situ Spectroelectrochemical Studies on the Reduction of Sulfur in Dimethyl Sulfoxide Solutions, J. Electrochem. Soc. 140 (1993) 115.

[46] X. Yu, A. Manthiram, A class of polysulfide catholytes for lithium–sulfur batteries: energy density, cyclability, and voltage enhancement, Phys. Chem. Chem. Phys. Phys. Chem. Chem. Phys. 17 (2015) 2127–2136.

[47] M.U.M. Patel, R. Demir-Cakan, M. Morcrette, J.M. Tarascon, M. Gaberscek, R. Dominko, Li-S battery analyzed by UV/vis in operando mode, ChemSusChem. 6 (2013) 1177–1181.

[48] D. Han, B. Kim, S. Choi, Y. Jung, Time-Resolved In Situ Spectroelectrochemical Study on, J. Electrochem. Soc. 151 (2004) E283–E290.

[49] M. Wild, L. O'Neill, T. Zhang, R. Purkayastha, G. Minton, M. Marinescu, G.J. Offer, Lithium sulfur batteries, a mechanistic review, Energy Environ. Sci. 8 (2015) 3477–3494.

FIGURES

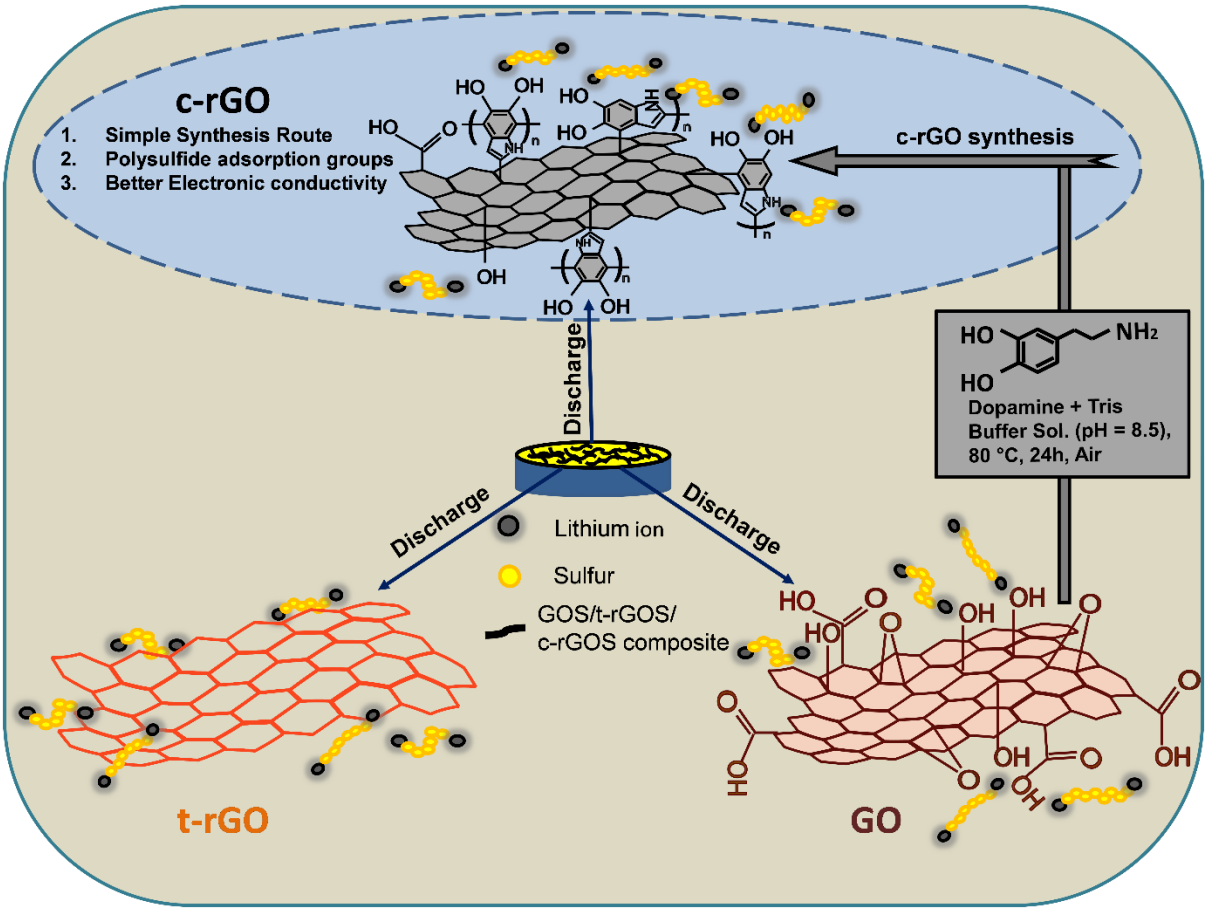

Fig. 1. Schematic illustration of the synthesis route of c-rGO carbon host along with the possible advantages of c-rGO carbon host over GO and t-rGO for polysulfide adsorption.

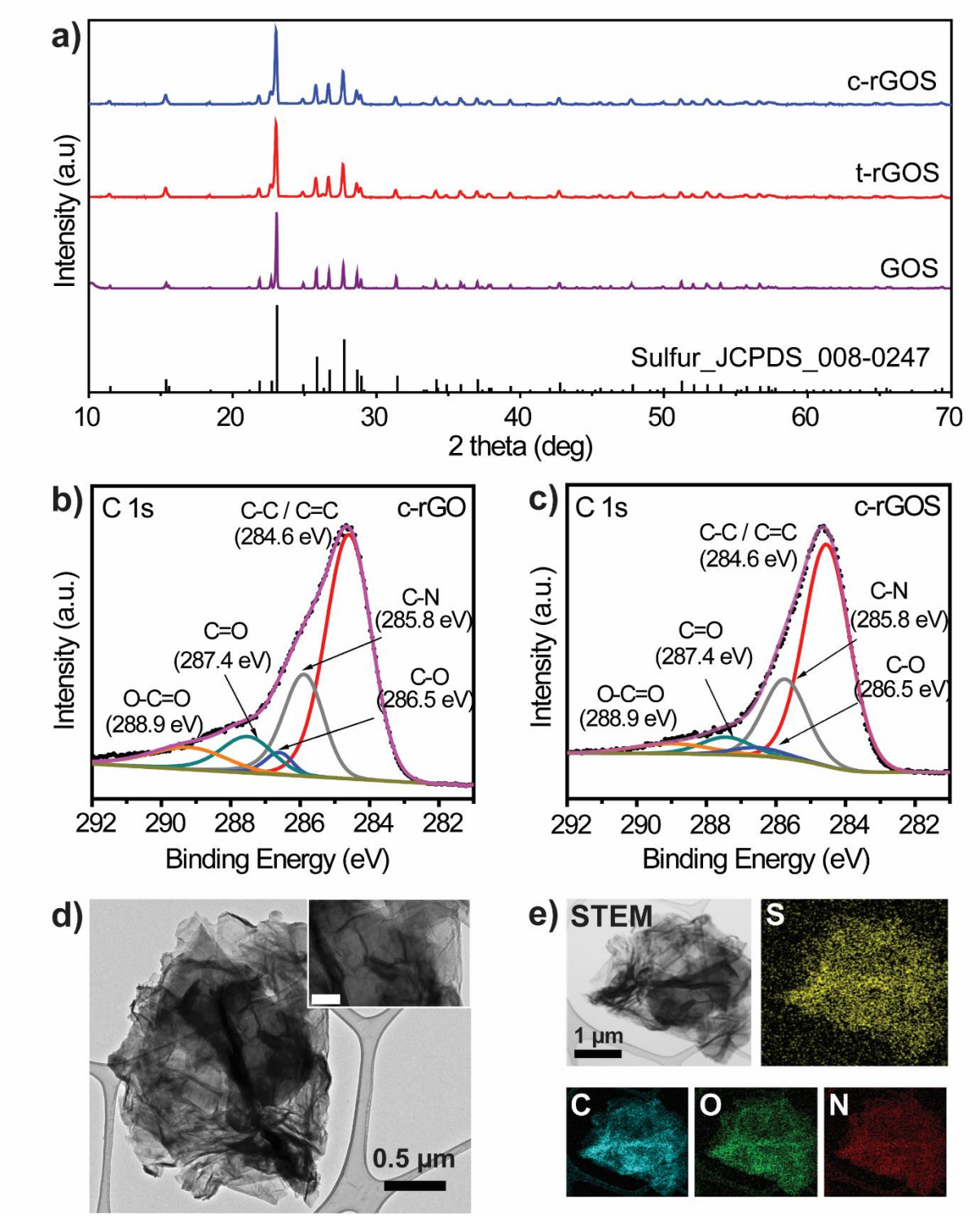

Fig. 2. (a) XRD analysis of GOS, t-rGOS and c-rGOS sulfur composites. (b, c) XPS deconvolution data of C 1s spectra of c-rGO and c-rGOS. (d, e) TEM and elemental mapping of c-rGOS composite. (The white bar in inset represents 200 nm scale)

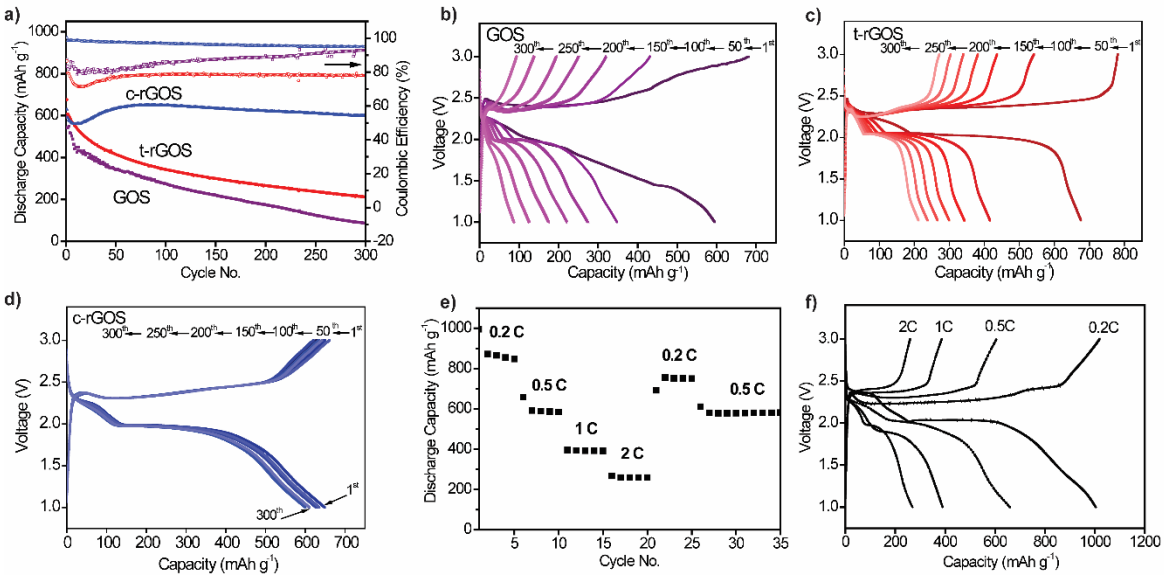

Fig. 3. (a) Cyclic performance of GOS, t-rGOS and c-rGOS at 0.5 C cycled between 3.0 V to 1.0 V upto 300 cycles. Corresponding voltage-capacity profile of (b) GOS, (c) t-rGOS and (d) c-rGOS at various cycles. (e) Rate capability of c-rGOS cycled between 0.2 C - 2 C (f) Corresponding 1st charge/discharge voltage–capacity profile at various C-rates.

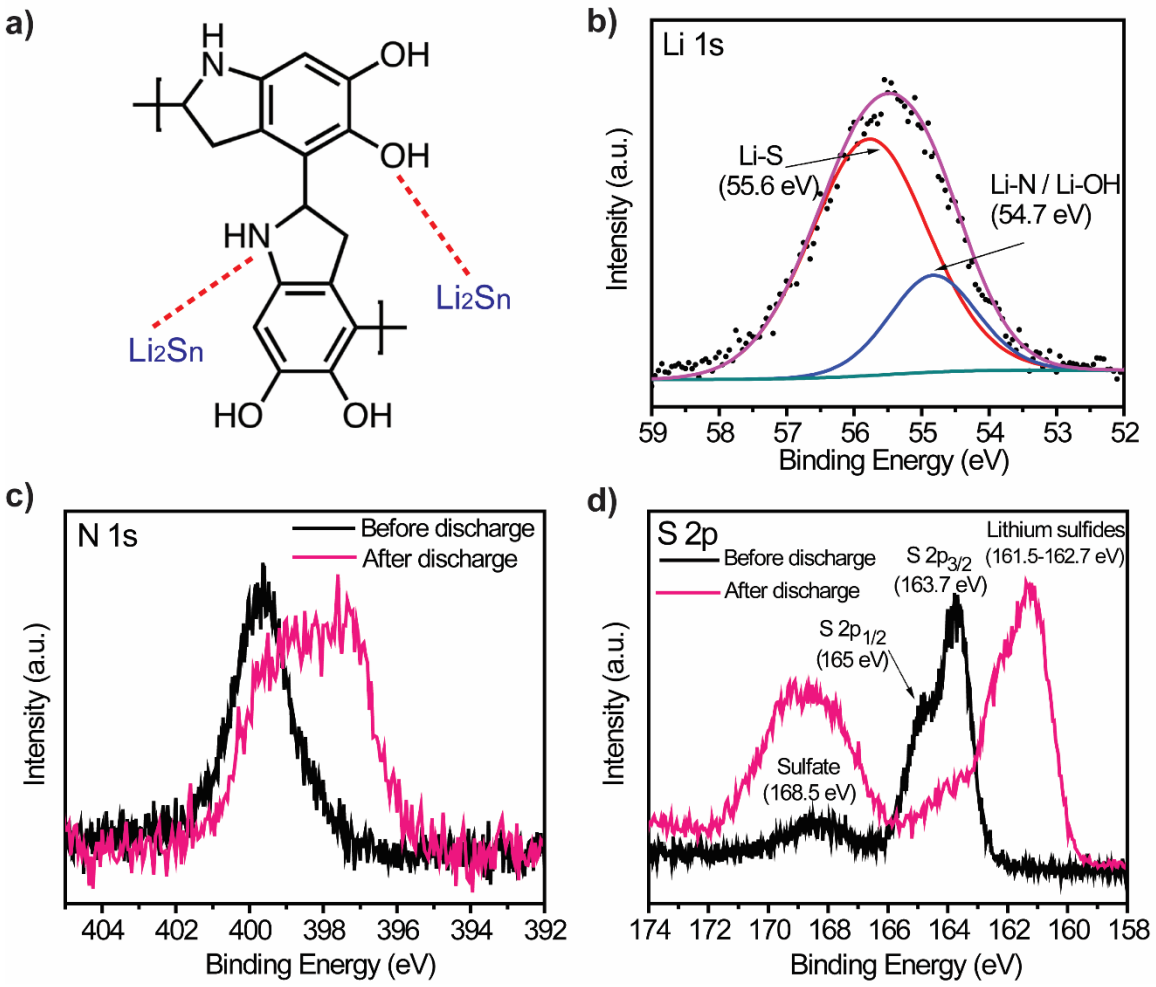

Fig. 4. (a) Schematic illustration of possible interaction between polysulfides & polydopamine functional groups. XPS spectra of (b) Li 1s after 1st discharge, (c) N 1s and (d) S 2p spectra before and after 1st discharge.

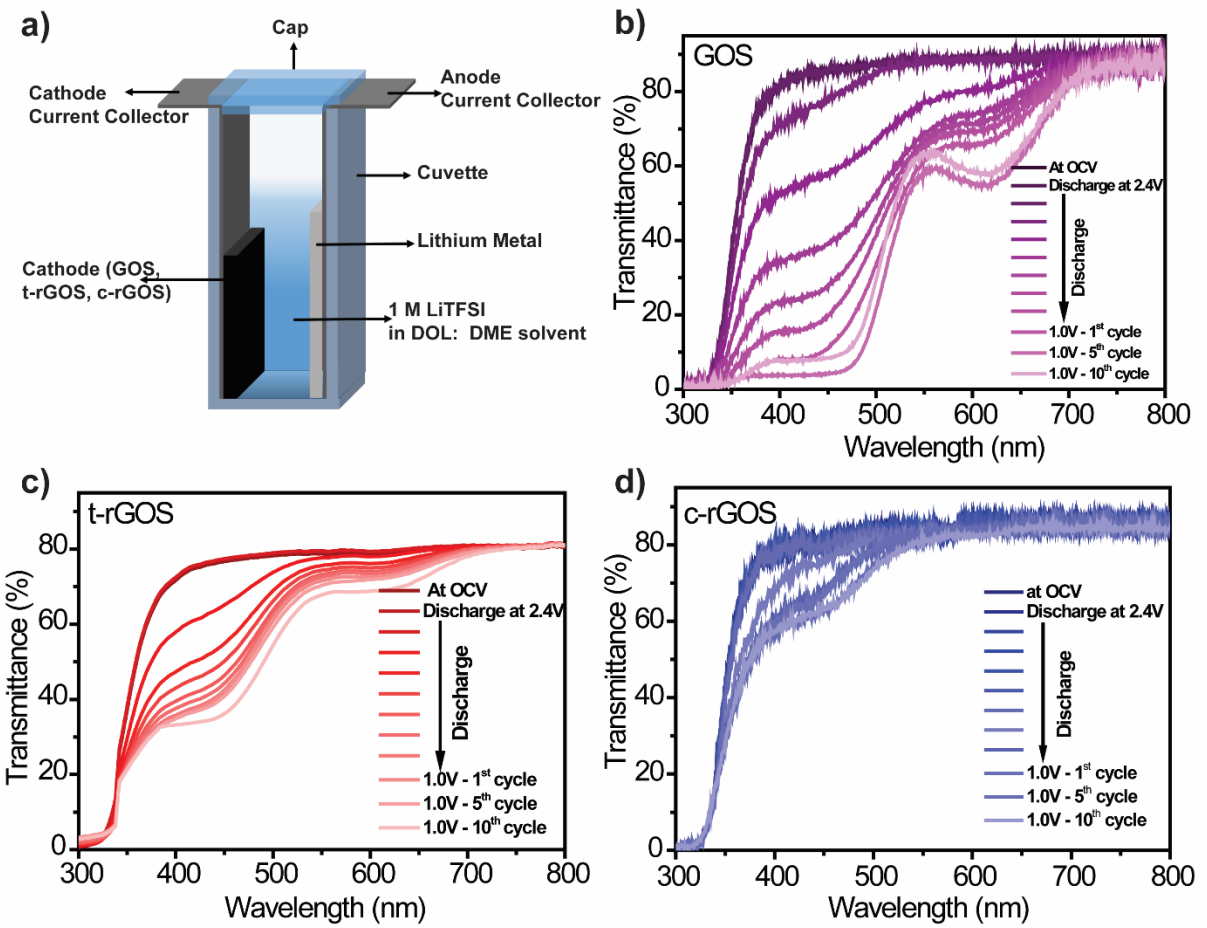

Fig. 5. (a) Schematic illustration of *in-situ* UV-Vis cuvette cell. Transmittance profile of (b) GOS, (c) t-rGOS and (d) c-rGOS *in-situ* cell during 1st, after 5th and 10th discharge at 0.05C.

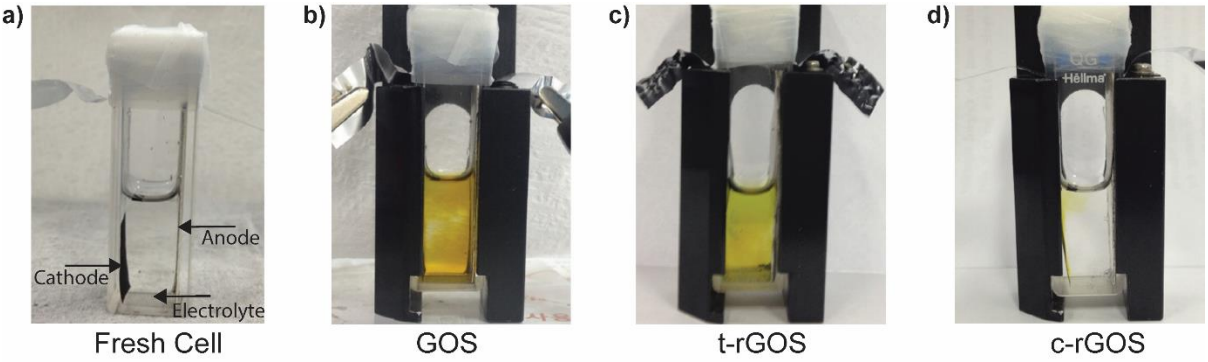

Fig. 6. (a) *In-situ* UV-Vis cell before 1st discharge. *In-situ* cell showing polysulfide dissolution in (a) GOS, (b) t-GOS and (c) c-rGOS *in-situ* cell after 10th discharge at 0.05 C. Minimal polysulfide dissolution can be seen in c-rGOS as compared to GOS and t-rGOS *in-situ* cell.